Human Molecular Genetics, 2009, Vol. 18, No. 14 **2643–2655**
doi:10.1093/hmg/ddp206
Advance Access published on May 4, 2009

X-linked cataract and Nance-Horan syndrome are allelic disorders

Margherita Coccia[1], Simon P. Brooks[1], Tom R. Webb[1], Katja Christodoulou[1], Izabella O. Wozniak[1], Victoria Murday[2], Martha Balicki[3,†], Harris A. Yee[3,†], Teresia Wangensteen[4], Ruth Riise[5], Anand K. Saggar[6], Soo-Mi Park[7], Naheed Kanuga[1], Peter J. Francis[1,†], Eamonn R. Maher[8], Anthony T. Moore[1,9], Isabelle M. Russell-Eggitt[10] and Alison J. Hardcastle[1,*]

[1]UCL Institute of Ophthalmology, London, UK, [2]Department of Clinical Genetics, Yorkhill Hospital, Glasgow, UK, [3]Division of Clinical and Metabolic Genetics, The Hospital for Sick Children, Toronto, Canada, [4]Department of Medical Genetics, Ullevål University Hospital, Oslo, Norway, [5]Department of Ophthalmology, Innland Hospital, Elverum, Norway, [6]St George's Hospital, London, UK, [7]Addenbrooke's Hospital, Cambridge, UK, [8]West Midlands Regional Genetics Service, Birmingham Women's Hospital, Birmingham, UK, [9]Moorfields Eye Hospital, City Road, London, UK and [10]Ulverscroft Vision Research Group, Great Ormond Street Hospital for Children, London, UK

Received February 19, 2009; Revised April 7, 2009; Accepted April 28, 2009

Nance-Horan syndrome (NHS) is an X-linked developmental disorder characterized by congenital cataract, dental anomalies, facial dysmorphism and, in some cases, mental retardation. Protein truncation mutations in a novel gene (*NHS*) have been identified in patients with this syndrome. We previously mapped X-linked congenital cataract (CXN) in one family to an interval on chromosome Xp22.13 which encompasses the *NHS* locus; however, no mutations were identified in the *NHS* gene. In this study, we show that NHS and X-linked cataract are allelic diseases. Two CXN families, which were negative for mutations in the *NHS* gene, were further analysed using array comparative genomic hybridization. CXN was found to be caused by novel copy number variations: a complex duplication–triplication re-arrangement and an intragenic deletion, predicted to result in altered transcriptional regulation of the *NHS* gene. Furthermore, we also describe the clinical and molecular analysis of seven families diagnosed with NHS, identifying four novel protein truncation mutations and a novel large deletion encompassing the majority of the *NHS* gene, all leading to no functional protein. We therefore show that different mechanisms, aberrant transcription of the *NHS* gene or no functional NHS protein, lead to different diseases. Our data highlight the importance of copy number variation and non-recurrent re-arrangements leading to different severity of disease and describe the potential mechanisms involved.

INTRODUCTION

Nance-Horan syndrome (NHS) is an X-linked cataract–dental syndrome (OMIM 302350) characterized by bilateral congenital cataract (usually requiring early surgery in affected males) associated with microcornea and microphthalmia, multiple dental anomalies and characteristic facial features (1,2). Dental abnormalities include Hutchinsonian incisors (screwdriver-shaped incisors), supernumerary maxillary incisors and widely spaced teeth (diastema) (1–3). Associated facial features include prominent nose and nasal bridge, long face and large ears with anteverted pinnae. A proportion of affected males (~30% of cases) have developmental delay (1–7). Carrier females typically display posterior Y-sutural lens opacities often with cortical riders that are likely to be congenital, whereas the dental and facial anomalies of the

*To whom correspondence should be addressed at: UCL Institute of Ophthalmology, 11-43 Bath Street, London, EC1V 9EL, UK. Tel: +44 2076086945; Fax: +44 2076084002; Email: a.hardcastle@ucl.ac.uk
†Present address: M.B.: BC Women's and Children's Hospital, Vancouver, Canada; H.A.Y.: The Genetics Clinic, Calgary, Canada; P.F.: Casey Eye Institute, Portland, OR, USA.

syndrome may be observed, but with a milder presentation (8). The minimal locus for this syndrome was mapped on Xp22, and subsequently mutations were identified within the coding exons of a novel gene, *NHS* (9–12). The *NHS* gene is alternatively spliced and composed of at least 10 coding exons with at least 3 isoforms (Supplementary Material, Fig. S1). Isoform A (*NHS-A*) has eight exons encoding a 1630-amino acid protein with an unusually large intron 1 (~350 kb); isoform B (*NHS-B*) is transcribed from exon 1b and translated from exon 4 encoding a 1335-amino acid protein; and isoform C (*NHS-C*) is transcribed and translated from exon 1a coding for a 1453-amino acid protein (11,13). To date, 18 pathogenic mutations have been identified in 4 of the 10 coding exons of the *NHS* gene, all of which are predicted to result in a truncated NHS protein (11,12,14–18). Isoform A is thought to be important in the pathogenesis of NHS, because patient mutations identified in exon 1 are only predicted to affect this isoform (11,12) (Supplementary Material, Fig. S1). The function of the NHS protein is unknown (13).

Non-syndromic X-linked congenital cataract is characterized by bilateral total nuclear cataract in affected males and Y-sutural opacities in carrier females (19–22). Early studies reported linkage with the Xg blood group on Xp22 (20). We previously described a four-generation family with X-linked congenital cataract (CXN) and mapped the disease locus to an ~3.5 Mb interval on Xp22.13 (23,24). This family did not exhibit the dental phenotype and facial dysmorphology of NHS; however, four of the six affected males also had congenital cardiac anomalies. The disease locus for this family mapped to the same critical region as NHS, suggesting allelic heterogeneity; however, mutation screening of the *NHS* gene failed to identify the cause of disease (12,23,24). The NHS critical interval is also syntenic with the mouse congenital cataract disease locus *Xcat* (X-linked cataract) (25,26). The *Xcat* mutation is characterized by congenital total lens opacities present at eye opening in both hemizygous males and homozygous females, whereas in heterozygous carrier females, the phenotype varies from barely noticeable to totally opaque lenses, similar to the cataract phenotype of NHS patients. The *Xcat* mouse was found to have a 487 kb insertion in intron 1 of the mouse *Nhs1* gene (27).

In this report, we describe a clinical and molecular analysis of seven families diagnosed with NHS and two families with X-linked cataract. All mutations causing an NHS phenotype are null mutations predicted to produce no functional protein. Our comparative genomic hybridization and subsequent molecular analyses revealed novel copy number variations of the *NHS* gene leading to cataract, demonstrating for the first time that NHS and X-linked cataract are allelic diseases.

RESULTS

The majority of cases are described as classic NHS; however, some clinical variability was observed in this patient group. Pedigrees are shown in Figure 1 and a more detailed description of clinical findings is shown in Table 1.

NHS patients and mutations

Family A. Affected male II:1 had congenital nuclear lens opacities and characteristic facial dysmorphism, and at age 4, typical dental anomalies were seen (Table 1). The proband's mother, I:1, had similar facial features and bilateral fine white dots in the posterior Y-sutures of her lenses, typical of a carrier female lens (Fig. 2A). *NHS* gene screening revealed a novel single-nucleotide substitution in exon 1, c.C472T, which is predicted to result in a nonsense mutation at p.Gln158X (Fig. 3). The introduction of a nonsense mutation in exon 1 of the *NHS* gene is predicted to result in no expression of the major isoform of NHS, isoform A.

Family B. Proband II:3 was diagnosed with bilateral congenital cataract and microphthalmia, typical dysmorphic features and moderately delayed mental development (Table 1). He had NHS dental anomalies including broad diastema mediale, hyperplastic labial frenulum, screwdriver-shaped incisors (Fig. 2B) and hypoplastic enamel (Fig. 2C). Sequencing of the *NHS* gene in affected male (II:3) revealed a novel frameshift mutation in exon 2. A deletion of 1 bp (c.614delC) (Fig. 3) at the second position of codon 205 alters the reading frame and is predicted to result in a premature stop codon following the addition of 77 amino acid, p.Pro206fsX282. Segregation analysis was performed to test for carrier status in the proband's asymptomatic mother (I:1) and his sisters (II:1 and II:2, Fig. 1B). The mutation in proband II:3 is considered to be a *de novo* mutation as it was identified only in the affected male.

Family C. Two affected brothers (II:1 and II:2, Fig. 1C) were diagnosed with NHS. Individual II:1 was diagnosed with dense central cataracts and small corneas with characteristic dental abnormalities (Fig. 2D). His older affected brother (II:2) displayed similar ocular phenotype (Table 1). Their mother (I:1) had typical carrier posterior Y-sutural opacities (Fig. 2E) and undiagnosed impacted teeth. Screening of the *NHS* gene revealed a nonsense mutation in exon 3. A C>T transition (c.C742T) (Fig. 3) at the first position of codon 248 alters the amino acid sequence from an arginine to a stop codon, p.Arg248X. The introduction of a nonsense mutation in exon 3 of the *NHS* gene is predicted to result in a severely truncated protein product. This mutation has been previously reported (18).

Family D. Individual II:1 was diagnosed with bilateral microphthalmia and congenital cataract as well as typical NHS dental anomalies and facial dysmorphism (Table 1). He also had mild bilateral hearing loss, and computed tomography (CT) scans demonstrated inner-ear dysplasia. His mother (I:1) had a history of cataracts diagnosed in her 20s and dental extraction of multiple supernumerary teeth. Interestingly, we detected a C>T nonsense mutation (c.C742T, p.Arg248X) in proband II:1 (Fig. 3) and his carrier mother I:1, which was identical to the nonsense mutation we identified in Family C and to a previously described mutation (18).

Family E. This family consists of three affected males (II:1, III:2 and III:3) and two females of unknown status (II:2 and

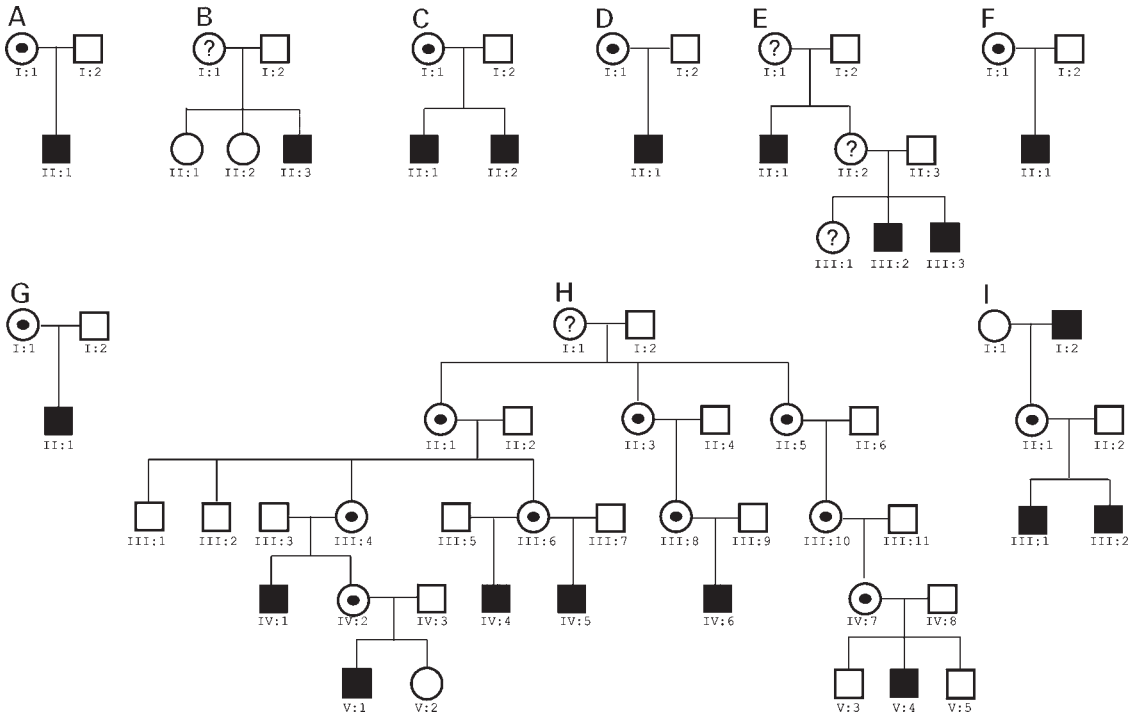

Figure 1. Pedigree structures. Families A, B, C, D, E, F and G were diagnosed with NHS. Families H and I were diagnosed with X-linked cataract. Black boxes denote affected males; dotted circles, carrier females; clear boxes and circles, unaffected individuals; and clear circles with a question mark, females with unknown clinical status.

III:1) (Fig. 1E). The proband, individual III:2, had bilateral congenital cataract and typical NHS dysmorphic features and dental anomalies, including screwdriver-shaped incisors (Fig. 2F). He was also diagnosed with finger and toe clinodactyly and behavioural problems. His affected brother (III:3) was diagnosed with bilateral cataract at age 2 and had a similar facial, dental and behavioural phenotype (Table 1). Their affected uncle (II:1) also had typical features of NHS. Screening of the *NHS* gene in the affected male (III:2) revealed a novel frameshift mutation in exon 6. A deletion of 4 bp (c.2550–2553delAGAA) (Fig. 3) at the third position of codon 850 alters the reading frame and is predicted to result in a premature stop codon following the addition of 3 amino acid, p.Lys850fsX852. The proband's mother (II:2) and sister (III:1) were both heterozygous for this sequence change.

Family F. Individual II:1 was diagnosed with dental anomalies, dysmorphic facial features and developmental delay, but with an unusually mild cataract for NHS (Fig. 2G and Table 1). His mother (I:1) had typical carrier features of NHS with asymptomatic cataract of very fine dots in a posterior Y-shaped distribution. Her teeth were also anomalous with poor enamel.

All coding exons of the *NHS* gene were successfully amplified and sequenced, except for exon 8. To understand why it was not possible to amplify exon 8, a chromosome walking strategy was adopted. Three exon 8 specific primers were designed: *NHS*Ex8ext, *NHS*Ex8 and *NHS*Ex8a (Supplementary Material, Table S1). Using primer pair *NHS*Ex8a/Uni, a unique fragment of ~700 bp was amplified. The PCR product was gel-purified and sequenced to reveal an insertion at the first position of codon 1521 (c.4561) (Fig. 3). Bioinformatic analysis of the sequence from patient II:1 revealed a genomic re-arrangement which affects the majority of *NHS* exon 8 coding sequence and the 3′-UTR. The *NHS* gene is truncated within exon 8 at position c.4561, and the deleted region extends another 4.3 kb to include sequence upstream of the neighbouring *SCML1* gene. The breakpoint junction also contains an insertion of a 17 bp fragment from the opposite (−) strand (Fig. 4A). Thus, a novel mutation in exon 8 was detected, which is the first NHS chromosomal re-arrangement described and is predicted to result in a premature stop codon with the addition of 11 aberrant amino acid, p.Ser1521fsX1531 (Fig. 3). A diagnostic PCR reaction was designed, using primer pair NHSEx8CR (Supplementary Material, Table S1), which successfully confirmed the presence of the chromosome re-arrangement in patient II:1 and its absence from 200 controls. Sequence analysis of the junction fragment revealed features similar to a previously described genomic re-arrangement in LIS1 (28), suggesting that this complex re-arrangement may be caused by a recently described mechanism of replication named fork stalling and template switching (FoSTeS) (29).

Family G. Affected male II:1 had bilateral congenital cataract, microphthalmia, dental anomalies, dysmorphism and developmental delay (Fig. 2H and Table 1). In addition to the typical features of NHS, individual II:1 was reportedly a 'floppy baby' and remained hypotonic. *NHS* gene exons failed to amplify in patient II:1 DNA. The patient DNA sample integrity was further tested with other primer pairs elsewhere on the X-chromosome, which amplified successfully. *NHS* exon 1 was

Table 1. Clinical features of individuals from study families

Family ID	Individual	Ophthalmological	Dental	Developmental delay and behavioural problems	Dysmorphism	Other
A	I:1	Bilateral fine white dots in the Y-suture of the lenses Cortical wedge opacities Optic discs with large cup-to-disc ratio (0.8 bilaterally) No evidence of glaucoma	—	—	Large ears and anteverted pinnae	—
	II:1	Bilateral small corneas (8.5 mm diameter) Irides lacking crypts Congenital white Y-sutural lens opacities Nuclear lens opacities with diffuse edge and clear peripheral lens Lensectomy was performed within the first month Both optic discs have large cups (0.6 right, 0.5 left) No evidence of glaucoma	Typical anomalies were seen at age of 4	—	Large ears and anteverted pinnae at 1 month	—
B	II:3	Bilateral congenital dense cataract Microphthalmia Extracapsular cataract extraction to clear pupil area and anterior vitrectomy was performed at 7 weeks of age and high plus contact lenses were fitted simultaneously Secondary glaucoma	Diastema mediale Hyperplastic labial frenulum Screwdriver-shaped incisors Hypoplastic enamel	Moderately delayed mental development Impaired social skills Not able to write or draw at age 8	Long thin face Large protruding ears	Delayed motor development
C	I:1	Posterior Y-sutural opacities	Undiagnosed impacted teeth	No	—	—
	II:1	Dense central cataracts Small corneas (horizontal corneal diameter 8.5 mm) at 12 days Underwent bilateral lensectomy at 2.5 weeks and wore contact lenses from 4 weeks	Characteristic dental abnormalities	No	Prominent ears	—
	II:2	Congenital cataracts Small corneas Bilateral posterior lenticonus Aphakic glaucoma and suffered an expulsive haemorrhage at trabeculectomy surgery Nystagmus	—	No	—	—
D	I:1	Cataracts diagnosed in her 20s	Dental extraction of multiple supernumerary teeth	No	—	—
	II:1	Bilateral microphthalmia, Congenital cataract, Ptosis Secondary glaucoma.	Peg-shaped teeth Supernumerary incisors	No	Facial dysmorphism	Bilateral hearing loss CT scans demonstrated inner-ear dysplasia.
E	II:1	Bilateral congenital cataract.	Typical dental anomalies	Developmental delay	—	—
	III:2	Bilateral congenital cataract.	Screwdriver-shaped incisors	Behavioural problems	Facial dysmorphism	Finger and toe clinodactyly
	III:3	Bilateral cataract at age 2	Typical dental anomalies	Behavioural problems	Facial dysmorphism	—

Continued

Table 1. *Continued*

Family ID	Individual	Ophthalmological	Dental	Developmental delay and behavioural problems	Dysmorphism	Other
F	I:1	Asymptomatic cataract of very fine dots in a posterior Y-shaped distribution Large cupped optic discs without glaucoma	Anomalous teeth with poor enamel	—	—	—
	II:1	Eye test failed at 7 years 8 months with an acuity of LogMAR 0.3 right, 0.26 left Unusually mild cataract At age 11, his corneas were slightly small, 10.5 mm Bilateral inferior wedge opacities in the lens cortex and fine nuclear dot opacities	Typical dental anomalies	Developmental delay and behavioural problems	Facial dysmorphism	—
G	II:1	Bilateral congenital cataract Microphthalmia A magnetic resonance imaging scan showed small anterior visual pathways and a general lack of bulk of white matter.	Typical dental anomalies	Developmental delay	Facial dysmorphism	Hypotonic
H	All males	Required cataract extraction in the first few months of life	No	No	No	Four out of six affected males were diagnosed with congenital heart defects (ductus arteriosus, tetralogy of Fallot, ventriculoseptal defect and stenosis of a major cardiac vessel)
	All females	Mild fan-shaped central nuclear opacities	No	No	No	—
I	II:1	Y-sutural lens opacities Her father had had cataract surgery at 45 years of age	No	No	No	—
	III:1	Dense bilateral nuclear cataracts at 6 weeks. Lensectomy was performed at 12 weeks and a posterior lenticonus found of the right lens. Both eyes had normal corneal diameter of 11 mm, axial lengths 18 mm right, 17.9 mm left, and no evidence of glaucoma. At 6 years of age, his acuity was 0.52 logMAR right and 1.3 LogMAR left with dense left amblyopia and no evidence of glaucoma	No	No	No	Laryngomalacia (inspiratory stridor) Pre-auricular pit
	III:2	Mild posterior sutural lens opacities, not operated on	No	No	No	Laryngomalacia (inspiratory stridor)

present, but all other *NHS* exons were deleted in this patient, which is predicted to result in no protein product (Fig. 3C). PCR analysis of the genes downstream of the *NHS* gene, *SCML1*, *RAI2*, *CXorf20* and *SCML2*, revealed an extensive segmental deletion of ~0.9 Mb. The deleted region encompasses the majority of the *NHS* gene (exons 2–8), *SCML1*, *RAI2* and *CXorf20* (Fig. 3C). The *SCML2* gene is not deleted in this patient (Fig. 3C).

Complex duplication–triplication event at the *NHS* locus and resulting phenotype

The phenotype for Family H has been previously reported as X-linked cataract (CXN) without the features of NHS (19). In brief, all affected males required cataract extraction in the first few months of life. Carrier females had mild fan-shaped central nuclear opacities (19). Features typical of NHS such

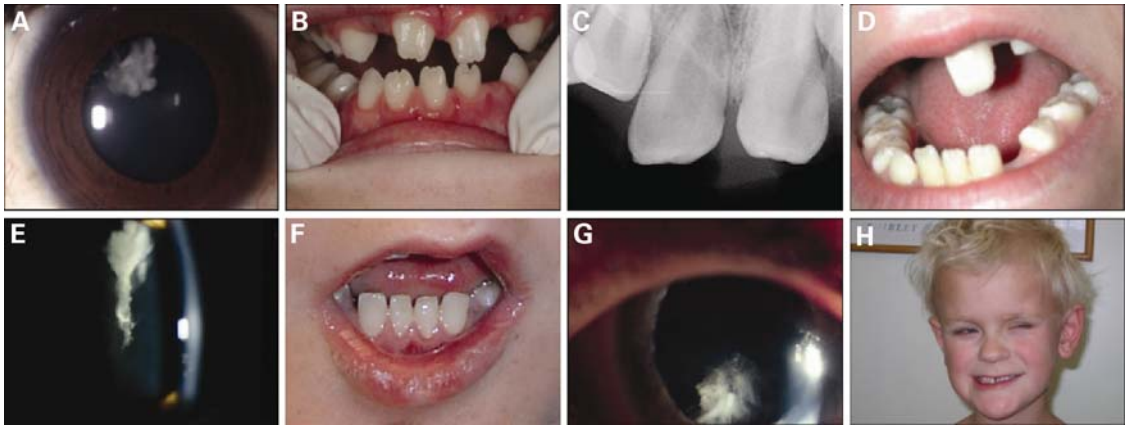

Figure 2. Patient phenotypes. (**A**) Carrier cataract phenotype (I:1) of Family A. (**B**) Family B dental phenotype (II:3) showing screwdriver-shaped incisors and broad diastema mediale with hyperplastic frenulum mediale and (**C**) hypoplastic enamel. (**D**) Family C proband (II:1) with dental anomalies and (**E**) sutural cataract phenotype of carrier mother (I:1). (**F**) Family E proband (III:2) with screwdriver-shaped incisors. (**G**) Relatively mild cataract phenotype of affected male (II:1) in Family F. (**H**) Typical features of NHS in affected male II:1 from Family G.

as dental anomalies, dysmorphism and developmental delay were not described in this family; however, congenital heart defects with a variety of diagnoses (ductus arteriosus, tetralogy of Fallot, ventriculoseptal defect and stenosis of a major cardiac vessel) were reported in four out of six affected males at the time of clinical examination. Genetic linkage studies in this family had previously shown that CXN was linked to the *NHS* locus (19,20). All coding exons of the *NHS* gene were successfully amplified and sequenced and no mutations were identified (12). Here, we describe the analysis of DNA from an affected male (IV:4) for copy number variation using a dense X-chromosome array.

Comparative genomic hybridization array data analysis revealed the presence of a complex re-arrangement consisting of triplication of a region encompassing *NHS*, *SCML1* and *RAI2* genes embedded within a duplicated region (Fig. 5A). The mean $\log_2$ ratio indicates that an $\sim$0.5 Mb region between ChX:17334242 and ChX:17800551 is triplicated, flanked by a duplication that extends 0.2 Mb distal and 0.1 Mb proximal to the identified triplication (Fig. 5A). To validate the presence of a triplicated region, a SYBR-green quantitative real-time PCR (qPCR) experiment was performed on four family samples: DNA from affected males IV:1 and IV:4 and DNA from unaffected males III:2 and V:3. Using primer pair NHSEx8c (Table S1) located within the triplicated region, the number of amplified copies of DNA for the affected males reaches the fluorescence threshold with a smaller C_T value compared with the number of amplified copies of DNA for the unaffected males. The results obtained from Data Analysis for Real-Time PCR (DART-PCR) are shown in Figure 5B, and the R_o values averaged for controls and patients show a significant increase of 2.8-fold in the two affected males compared with the two unaffected males.

The triplicated region includes the *NHS* gene lacking exon 1, and the entire *SCML1* and *RAI2* genes. To define the breakpoint regions of this complex re-arrangement, a chromosome walking strategy was used. Three target-specific primers (TSPs) were designed in the breakpoint 3 region (Fig. 5A): Bk3F1, Bk3F2 and Bk3F3 (Supplementary Material, Table S1). Using primer pair Bk3F3/Uni, amplification of two products was detected. Direct sequencing of these products revealed that breakpoint 3 (at ChrX:17800261) joins sequence downstream of *RAI2* to sequence of unknown origin (Fig. 5C). The same strategy was used to define the proximal breakpoint (breakpoint 4, Fig. 5A). Additional TSPs, Bk4F1, Bk4F2 and Bk4F3 (Supplementary Material, Table S1), were designed in the proximal breakpoint region (breakpoint 4). Amplification of an $\sim$1.4 kb product was detected using primer pair Bk4F3/Uni. Direct sequencing of this product revealed that breakpoint 4 (at ChrX:17926944) joins sequence downstream of the *RAI2* gene to sequence upstream of exon 1 of the *NHS* gene (ChrX:17105038) (Fig. 5C). Attempts to walk across distal breakpoint 2 located between ChrX:17104696 and ChrX:17105121 were not successful, and walking across distal breakpoint 1 located between ChrX:17334022 and ChrX:17334242 was not performed.

Sequence analysis of breakpoint 4 also revealed the presence of 'mirrored' sequences at both the distal and proximal re-arrangement boundaries (Fig. 4B). This breakpoint occurs in sequence which is conserved across species (Fig. 4D) and is possibly a promoter region for the *NHS* gene. Disruption of this conserved upstream region is predicted to affect the transcription of one copy of the *NHS* gene. Therefore, we conclude that one copy of the *NHS* gene lacks exon 1 (Fig. 5A), another copy has all known exons but is disrupted upstream, and a third copy is intact. The three copies of the *SCML1* and *RAI2* genes appear complete. The additional phenotype of congenital heart defects observed in some affected males could be due to perturbed *NHS* gene transcription or increased dosage of the *NHS, SCML1* or *RAI2* genes. Segregation of the complex copy number variation in Family H was confirmed using primer pair CXN–Bk (Supplementary Material, Table S1) designed to amplify across breakpoint 4 of the segmental duplication–triplication (Fig. 5D). A PCR product of 338 bp representing successful amplification across the breakpoint was detected in all 10 affected and carrier individuals and not in unaffected members of Family H.

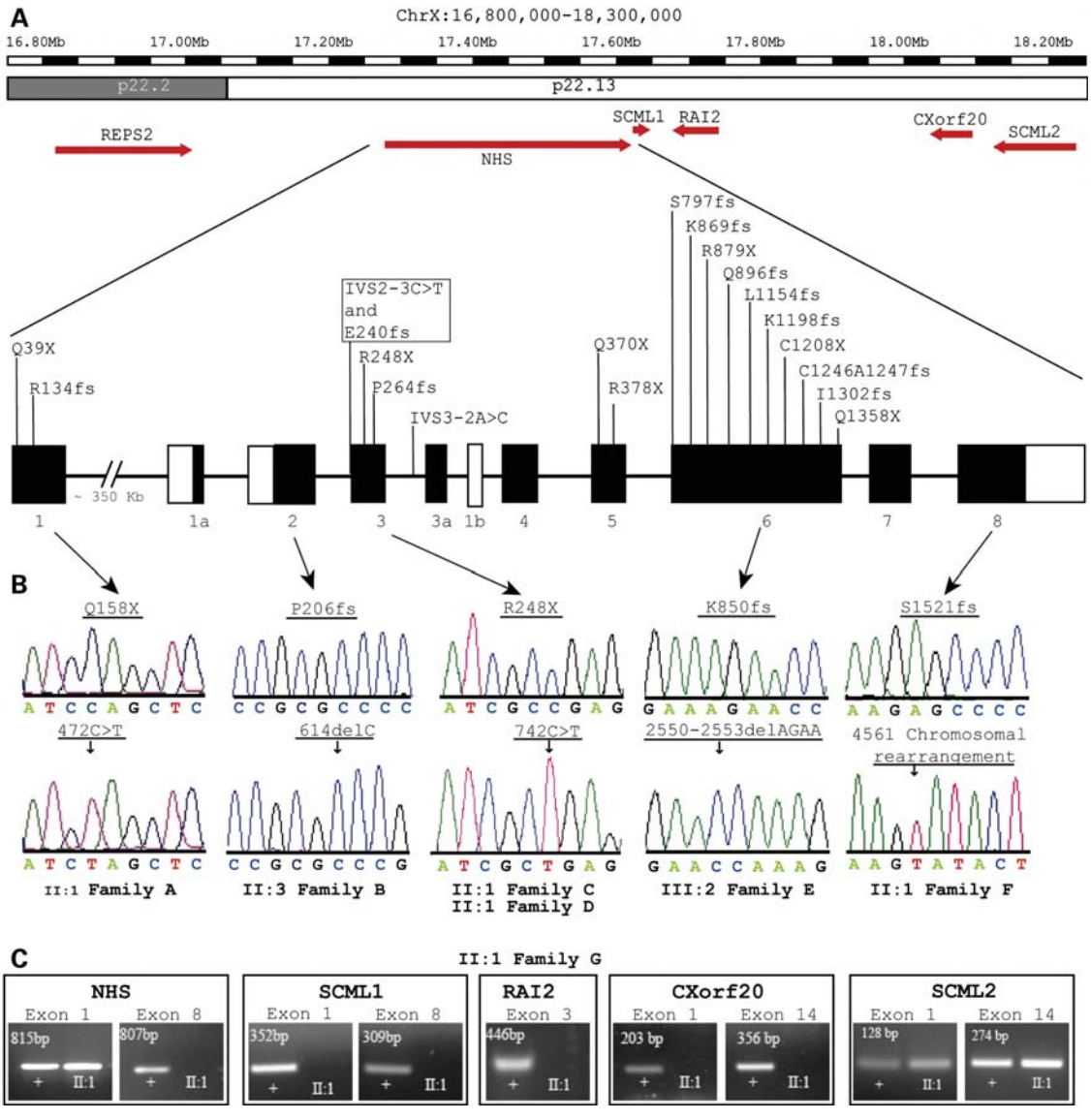

Figure 3. Patient mutations identified in the *NHS* gene. (**A**) Schematic representation of the X-chromosomal region surrounding the *NHS* gene (16.80–18.30 Mb). Arrows in red indicate position and direction of genes. Genomic structure of the *NHS* gene is shown with mutations identified to date. (**B**) Sequence chromatograms showing protein truncation mutations identified in Families A–F. Mutations detected in affected male sequence are shown below the unaffected control male chromatograms. (**C**) Agarose gels showing amplification of *NHS* exon 1a and *SCML2* exons 1 and 14 and absence of *NHS* exon 8, *SCML1* exons 1 and 8, *RAI2* exon 3, *CXorf20* exons 1 and 14 for the affected male in NHS Family G (II:1) compared with a control male (+). Corresponding amplicon sizes are indicated.

NHS intragenic deletion and resulting phenotype

Individual III:1 from Family I was diagnosed with dense bilateral nuclear cataracts at 6 weeks. At 2 months, there appeared to be no dysmorphic features characteristic of NHS. However, he did have a small pit in the right external ear in the ascending limb of the helix, which may be a small pre-auricular sinus. His older brother, individual III:2, shows no NHS features or pre-auricular sinus and had milder posterior sutural lens opacities, which were not operated on. Their mother (II:1) showed typical carrier Y-sutural lens opacities. Her father had cataract surgery at 45 years of age. There were no further details available of this individual. This family was therefore diagnosed as X-linked cataract. Laryngomalacia was also noted, which presented as inspiratory stridor in both boys. All of the *NHS* gene-coding exons and their splice sites were successfully amplified and sequenced. No mutation was identified in this family.

We then analysed DNA from individual III:1 for copy number variation using a dense X-chromosome array as described. Comparative genomic hybridization array data revealed the presence of an intragenic segmental deletion (Fig. 5E). The mean $\log_2$ ratio indicates that an ~5.1 kb region, between ChrX:17461256 and ChrX:17466720 located within the *NHS* gene, is deleted. Using primers pair *NHS*intron1 (Supplementary Material, Table S1), PCR amplification

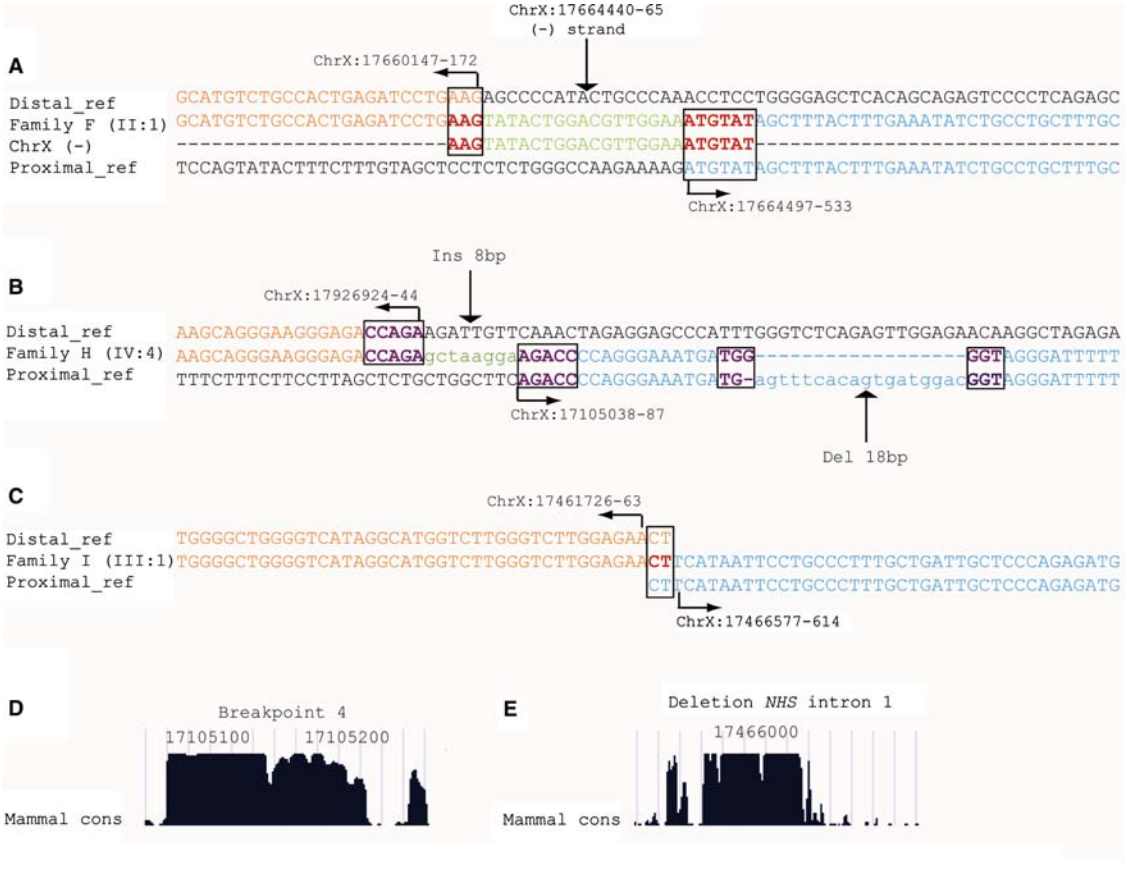

Figure 4. Sequence analysis of chromosome re-arrangements. Sequence analysis of breakpoint junctions of chromosome re-arrangements in Families F, H and I, and conserved regions in Families H and I. Normal distal genomic sequence is shown in orange on the top line; patient genomic breakpoint sequence is shown on the middle line; normal proximal genomic sequence is shown in blue on the bottom line. Chromosome positions are indicated along the sequences. (**A**) Chromosomal re-arrangement in Family F. A 17 bp fragment (green) between the distal and the proximal reference sequence is derived from the reverse strand in the intergenic region between *NHS* and *SCML1* genes. Regions of homology at the distal and proximal breakpoint sequences are boxed. (**B**) Breakpoint 4 of the complex duplication–triplication copy number variation in Family H. An insertion of 8 bp at the distal breakpoint (green) and an 18 bp deletion at the proximal breakpoint (blue dash) were detected. 'Mirrored' sequences at the distal and proximal breakpoint regions are boxed. (**C**) Deletion breakpoint in Family I shows identical nucleotides between the proximal and distal flanking sequence. A region of complete homology is boxed. (**D**) Breakpoint 4 in Family H occurs within a 240 bp sequence conserved across species. (**E**) Sequence conservation across species of a 340 bp region within the deletion in Family I.

of this region in the affected male (III:1) produced a smaller DNA fragment of 913 bp compared with a product of 5724 bp in an unaffected control sample (Fig. 5F). Sequence analysis revealed a 4.8 kb deletion within the large (~350 kb) intron 1 of the *NHS* gene (Fig. 5G). Analysis of the junctional sequence showed microhomology between the distal and proximal breakpoints, with 2 bp (CT) of perfect identity (Fig. 4C). The mechanism for this deletion could be either non-homologous end-joining (NHEJ) or a single FoSTes event. The intragenic region between ChrX:17465805 and ChrX:17466048 contains several highly conserved regions. The largest conserved region within the deletion is shown in Figure 4E and may be a regulatory sequence for the *NHS* gene. This deletion is therefore predicted to cause altered transcriptional regulation of the *NHS* gene.

DISCUSSION

In this study, we have identified several novel mutations in the *NHS* gene that cause NHS (Table 2). Importantly, we have also identified copy number variation of *NHS* in two families with X-linked cataract but without other features of NHS, revealing for the first time that NHS and X-linked cataract are allelic (Table 2). We suggest that lack of functional NHS protein causes NHS, whereas aberrant transcription of the *NHS* gene leads to a milder X-linked cataract phenotype.

We identified copy number variations of the *NHS* gene in two families with X-linked cataract, using array comparative genomic analysis (CGH). A segmental duplication–triplication encompassing the *NHS*, *SCML1* and *RAI2* genes (0.8 Mb) was identified in Family H, and a 4.8 kb deletion in *NHS* intron 1 was identified in Family I. This is the first report describing X-linked cataract phenotypes caused by copy number variation mutation. There is a striking difference in predicted mutational consequence leading to cataract or syndrome. NHS is caused by null mutations leading to non-functional NHS protein. X-linked cataract in the families described is likely to be caused by aberrant transcription of the *NHS* gene. This hypothesis is supported by our molecular analyses of two cataract families described in this study and also by the identification of the mutation causing X-linked cataract (*Xcat*) in a mouse model (27).

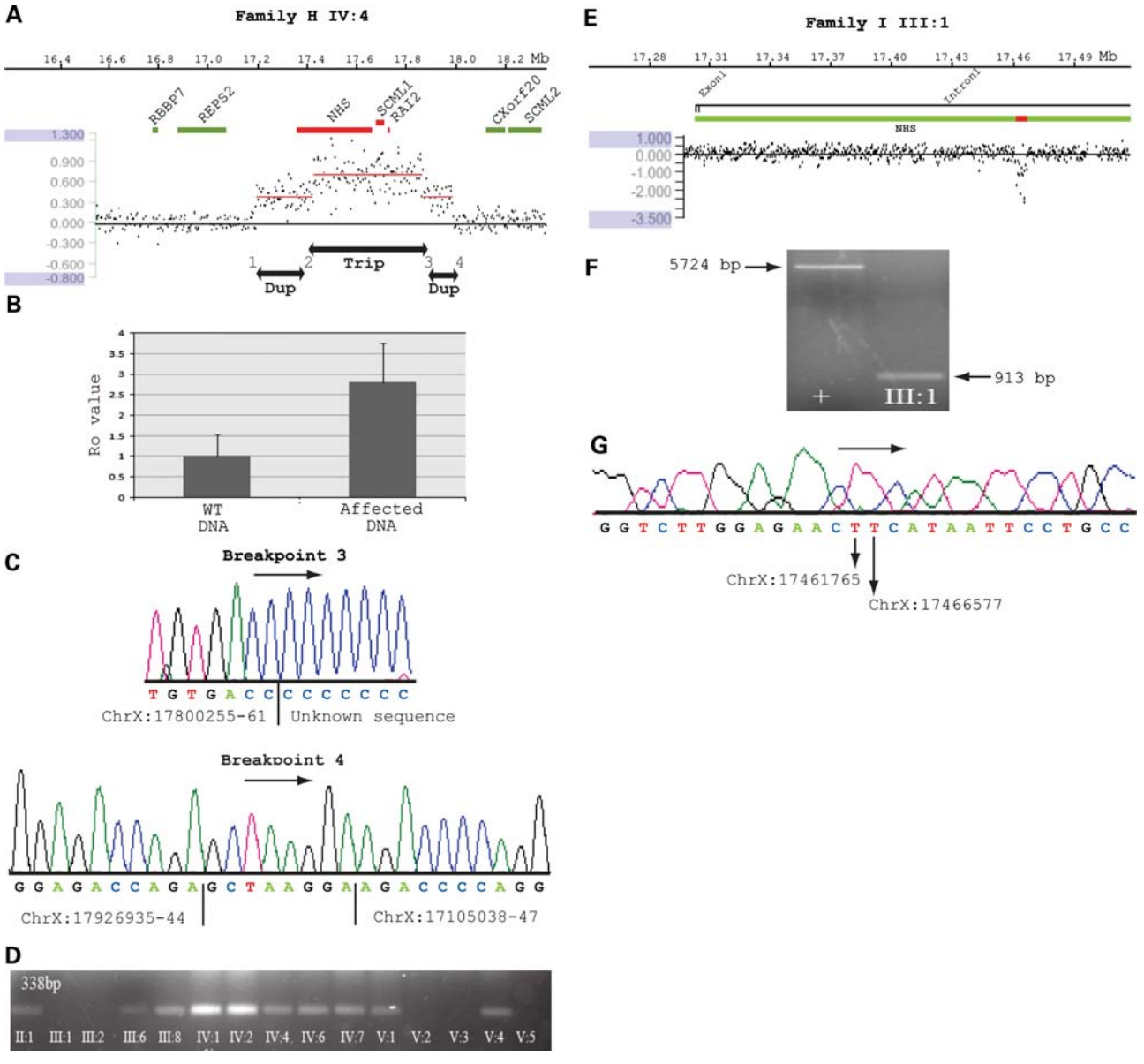

Figure 5. Copy number variations identified in CXN families. (**A**) Array CGH results from patient IV:4 in Family H. A complex duplication–triplication was found between ChX:17105121 and ChX:17926943. Position of the *NHS* gene and neighbouring genes are shown, and affected genes are highlighted in red. Genes present at normal copy number are shown in green. A schematic representation of the duplication–triplication region is shown below depicting breakpoint regions 1–4. (**B**) Relative quantification of qPCR data showing R_o values averaged between affected samples IV:1 and IV:4 normalized to R_o values averaged between WT samples III:2 and V:3. (**C**) Sequence derived from breakpoint 3 is shown with ChrX:17800261 joined to sequence of unknown origin, and sequence derived from breakpoint 4 is shown with ChrX:17926944 sequence joined to ChrX:17105038 sequence. (**D**) Genetic analysis of other relatives in the family demonstrated segregation of this complex re-arrangement in Family H with all affected and carriers individuals. (**E**) Array CGH results from patient III:1 in Family I. A deletion of a 4.8 kb region is located between ChrX:17461256 and ChrX:17466720. This deleted region is located within intron 1 of the *NHS* gene and is shown in red above the CGH data. (**F**) Agarose gel showing that PCR across the deletion breakpoint in affected male III:1 (CXN Family I) produces a 913 bp fragment compared with a control (+) fragment of 5724 bp. Fragment sizes are indicated. (**G**) Patient chromatogram showing the breakpoint sequence, which occurs at ChrX:17461765.

In CXN Family H, the segmental duplication–triplication breakpoint 4 occurs in a region located upstream of one copy of the *NHS* gene. This region is conserved across species (Fig. 4D). It is therefore likely that this region harbours important promoter sequence elements required for the spatial and temporal expression of *NHS* during development, and that disruption of the promoter leads to aberrant transcription of one copy of the *NHS* gene in the affected members of this family. Another copy of the *NHS* gene lacks exon 1; therefore, isoform A will not be expressed (Fig. 5A). The third copy of the *NHS* gene in affected members of this family may have preserved developmental expression control elements, however increased dosage of the transcript could also be a mechanism leading to CXN in affected members of the family.

In CXN Family I, a 4.8 kb deletion was detected within the unusually large intron 1 (~350 kb) of the *NHS* gene.

Table 2. Summary of mutations in the *NHS* gene

Family ID	*NHS* gene mutation and exon	Predicted consequence
A	c.C472T	p.Gln158X
	Exon 1	Protein truncation
B	c.614delC	p.Pro206fsX282
	Exon 2	Protein truncation
C	c.C742T	p.Arg248X
	Exon 3	Protein truncation
D	c.C742T	p.Arg248X
	Exon 3	Protein truncation
E	c.2550-2553del4bp	p.Lys850fsX852
	Exon 6	Protein truncation
F	c.4561	p.Ser1521fsX1531
	Intragenic genomic re-arrangement in exon 8	Protein truncation
G	Deletion of *NHS* gene downstream of exon 1	No protein product
H	Segmental duplication–triplication	Altered transcriptional regulation
I	Intragenic segmental deletion within intron 1	Altered transcriptional regulation

Interestingly, this deleted region also contains conserved sequences, which may represent potential promoter sequences, such that the deletion could lead to aberrant transcription of the *NHS* gene. This is supported by the fact that in the compact genome of Fugu, where gene density is high and introns are small (majority $<$150 bp) (30), the large *NHS* intron 1 is proportionally retained ($\sim$30 kb), suggesting the presence of functional elements. The hypothesis that intron 1 is important for transcriptional regulation is supported by the identification of the mutation in the *Xcat* mouse (27). The large size of *NHS* intron 1 is conserved in mouse (283 kb) and the *Xcat* mouse has a 487 kb insertional mutation in *Nhs* intron 1, resulting in a 770 kb separation of exons 1 and 2 (27). This led to the absence of expression of the major isoform of the *Nhs* gene which contains exon 1 (isoform A) (27). Collectively, the *Xcat* mouse mutation and phenotype, and our data indicating aberrant transcription of the *NHS* gene causes CXN, suggest that the *Xcat* mouse is an excellent model for CXN, but may not be a model for NHS. A knock-in mouse mutant of an NHS patient protein truncation mutation, or knock-out model, may lead to a dental phenotype, developmental delay and perhaps other symptoms associated with NHS.

Congenital heart defects were observed in four of six affected males in Family H (23). The additional phenotype in this family could be due to aberrant transcription of the *NHS* gene or increased dosage (triplicated) of the *NHS*, *SCML1* or *RAI2* genes. Retinoic acid-induced 2 protein (encoded by *RAI2*) is a good candidate, as retinoic acid is important for heart development (31). Developmental expression studies in mouse suggest that *Nhs* may also play a role in heart development (11). The mutation identified in NHS Family G supports the hypothesis that aberrant transcription of the NHS gene is responsible for congenital heart defects in CXN Family H. In Family G, we detected a segmental deletion which encompasses the majority of the *NHS* gene and the entire *SCML1*, *RAI2* and *CXorf20* genes. Despite the absence of these additional genes (*SCML1*, *RAI2* and *CXorf20*), Family G did not exhibit any cardiac abnormalities. It would appear therefore that aberrant transcription or a dosage effect of *NHS* leads to cardiac anomalies in Family H. Further support comes from a recent report describing a 2.8 Mb microdeletion of 16 genes on Xp22, including *NHS* and *RAI2*, with a phenotype of early seizures, severe encephalopathy, NHS and the congenital heart defect, tetralogy of Fallot (32). However, further work is required before one can assign heart defects in patients with specific genes affected by copy number variations on Xp22.

The intragenic re-arrangement detected in *NHS* exon 8 in Family F, segmental duplication–triplication in Family H and segmental deletion in Family I are non-recurrent genomic re-arrangements. We performed molecular analysis of breakpoints to determine the nature and mechanism of these genomic re-arrangements. In Family F, the chromosomal re-arrangement is likely to have occurred by the newly described mechanism of replication FoSTeS, as microhomology was detected at the junction breakpoints (29). In Family I, the segmental deletion occurred either by NHEJ or by a single FoSTeS event, as microhomology was also noted at the breakpoint junction; however, a precise mechanism could not be assigned. The duplication–triplication breakpoints 3 and 4 confirm two independent events leading to the complex re-arrangement observed with CGH in Family H. Breakpoint 4 appears to be caused by a new mechanism, as 'mirrored' sequences were identified at the junctional fragments. To our knowledge, the breakpoint sequence of only one other segmental duplication–triplication has been previously reported (28). In this article, the chromosomal re-arrangement encompasses a region on 17p13 in one patient with a developmental brain abnormality, but no mirrored sequences at the breakpoints were identified (28). We suggest, therefore, that novel mechanisms may be responsible for the re-arrangements identified in Families H and I which warrant further characterization.

Four novel protein truncation mutations, p.Q158X (exon 1), p.P206fs (exon 2), p.K850fs (exon 6), p.S1521fs (exon8), and a large deletion encompassing the majority of the *NHS* gene were identified in five of the seven NHS families. The two remaining NHS families, one from the UK (Family C) and one from Canada (Family D), were found to have the same protein truncation mutation p.R248X (exon 3). This mutation has also been identified in an Australian NHS family (18). Since the majority of NHS families described have a unique mutation, it is likely that these families are related. Referring clinicians confirmed that Families C and D are likely to be related, however their relationship with the Australian family previously described has not been confirmed. We have also identified a *de novo* mutation in exon 2 (p.P206fs) in one NHS patient and the first intragenic chromosomal re-arrangement causing NHS, which results in a frameshift mutation in exon 8 (S1521fs), predicted to result in a truncated, aberrant protein product. In addition, we identified a large deletion encompassing the majority of the *NHS* gene in Family G predicted to result in no NHS protein. This brings the total number of mutations identified in the *NHS* gene causing NHS to 23, all of which are null mutations (11,12,14–18). A summary of the clinical findings for each family is given in Table 1. All patients with null mutations

have the classic cataract and dental anomalies, which characterize NHS (1,2). Clinical variability also exists in our patient group. Given that Families C and D have the same mutation, one might expect clinical correlation; however, individual II:1 in Family D had bilateral mild hearing loss, with CT scans showing inner-ear dysplasia. This is the first report of an auditory phenotype associated with NHS. We found that UniGene cluster Hs.201623 has several NHS cDNA clones derived from fetal cochlea, suggesting that the gene may be important for the development of this organ. However, the fact that neither of the two affected boys in Family C suffers from hearing loss suggests that other genetic or environmental factors influence the phenotype. In our NHS patient cohort, developmental delay and behavioural problems were commonly observed (four out of seven NHS families, 57%), which we propose is also due to modifier effects influencing phenotype. Interestingly, no missense mutations in the *NHS* gene have been reported to date, which suggests that missense mutations do not cause disease, or that they lead to a more severe phenotype. Other loci and genes causing syndromic or isolated X-linked cataract have been described, for example Lowe syndrome on Xq26.1 and a locus on Xq24 (33,34). Further investigation of phenotypic variation and CNVs at these loci will enhance our understanding of phenotype–genotype correlation.

We have demonstrated that NHS and CXN are allelic disorders caused by different effects on *NHS* gene function and expression. Our data show the importance of copy number variation and non-recurrent re-arrangements leading to different severities of disease and describe the potential mechanisms involved. We have also shown that genetic or environmental modifiers of *NHS* gene function influence phenotype. Our study, taken together with the *Xcat* mouse study, indicates that the unusually large intron 1 of the *NHS* is important for gene regulation, and that the *Xcat* mouse is a model for X-linked cataract.

MATERIALS AND METHODS

Patients and clinical assessment

Patients diagnosed with NHS, or CXN, were ascertained in clinics in the UK, Canada and Norway. Informed consent was obtained from all individuals or their guardians and a blood sample taken for genomic DNA isolation. Where available, DNA from additional family members was collected. Family members were examined by clinical geneticists and/or ophthalmologists and family histories were taken. Of the nine families described (A–H), seven were diagnosed with NHS and two with CXN. Pedigree structures are shown in Figure 1. Pedigree H is an abridged pedigree of a previously described family (23,24), and part of Family C was previously described (11; Pedigree 6). All were consistent with X-linked inheritance and lacked a molecular diagnosis, however recessive inheritance could not be ruled out for Families B and E.

NHS gene screening

All *NHS* coding exons and their splice sites were amplified and sequenced directly from genomic DNA (see Supplementary Material, Table S2, for primers and conditions). ReddyMix™ PCR Master Mix (Abgene, Epsom, UK) was used for amplification with 2 pmol of each primer and 150 ng DNA. For *NHS* exon 1, Abgene Extensor Hi-Fidelity PCR Master Mix was used. PCR conditions were as follows: 95°C for 5 min, followed by 30 cycles at 95°C for 30 s, annealing temperature T_m (Supplementary Material, Table S2) for 30 s, and 72°C for 30–90 s, with a final extension at 72°C for 5 min. PCR products were purified using ExoSAP- IT® (USB), following manufacturer's protocols. Purified PCR products were sequenced using ABI BigDye terminator cycle sequencing chemistry version 3.1 on a 3730 DNA Analyzer (Applied Biosystem) following manufacturer's protocols. Patient DNA sequences were analysed using Lasergene software (DNASTAR Inc.). To verify the pathogenicity of the mutations identified, 200 control male DNA samples (i.e. 200 X-chromosomes) were tested. Specific primer pairs, incorporating the mutation detected, were designed to test control individuals (Supplementary Material, Table S1).

Comparative genomic hybridization

Array CGH was used to evaluate DNA copy number differences on the X-chromosome (performed by NimbleGen Systems Inc.). Male patient DNA was labelled with Cy-3, and a reference male DNA sample was labelled with Cy5. Affected individual IV:4 from CXN Family H and affected individual III:2 from CXN Family I were hybridized independently to a dense X-chromosome array with a median probe spacing of 340 bp. The data were visualized using SignalMap software (NimbleGen System Inc.). Array construction, labelling, hybridization, normalization and data analysis were performed at NimbleGen, and subsequent data analysis was performed in-house.

Chromosome walking

The isolation and characterization of unknown DNA sequence adjacent to known sequence were necessary for Families F and H. A Seegene DNA Walking SpeedUp™ Premix Kit (Biogene, UK) was used for genome walking following manufacturer's protocols. TSPs 1, 2 and 3 (Supplementary Material, Table S2) were designed to be used with DNA-walking ACP primer and Universal primer for primary, secondary and tertiary genome-walking amplification. The resulting tertiary PCR products were gel-separated, purified (QIAquick Gel Extraction Kit, Qiagen) and sequenced. Breakpoint sequences were analysed by comparison with reference sequences using tools available at UCSC and Ensembl genome browsers.

SYBR-Green qPCR assay

qPCR was performed using Power SYBR Green Mastermix (Applied Biosystems) on an Applied Biosystems 7900 HT Fast Real-Time PCR System. Each reaction was run in triplicate and contained 2× power SYBR Green master mix, 2 pmol of each primer and 100 ng DNA in a final reaction volume of 25 μl. Cycling conditions were as follows: 95°C for 10 min to activate the Amplitaq Gold polymerase, fol-

lowed by 40 cycles at 95°C for 15 s (denaturation) and 60°C for 1 min (annealing and extension). Dissociation curves were then generated by heat denaturation over a temperature gradient from 60–95°C to ensure no primer-dimers had formed and to check for a single amplicon. To verify the presence of a single PCR product, samples were also electrophoresed on a 2% agarose gel.

Data analysis

Data were obtained using SDS sequence detector 2.2.2 software (Applied Biosystems). Raw data exported from SDS 2.2.2 were analysed using DART-PCR (35). This workbook automatically calculates threshold cycles, amplification efficiency and resulting R_o values with the associated error.

SUPPLEMENTARY MATERIAL

Supplementary Material is available at *HMG* online.

ACKNOWLEDGEMENTS

The authors are grateful to all the families who participated in this study. We wish to thank Dr Jon Ruddle and Dr Cheryl Shuman for help with patient consent, Dr Hilde Nordgarden for oral examinations, Dr Jenny Mckenzie for help with the analysis of SYBR-Green qPCR data and Professor Mike Cheetham for comments on the manuscript.

Conflict of Interest statement. None declared.

FUNDING

This research was funded by Fight for Sight and The Wellcome Trust (077477/Z/05/Z). M.C. is a Fight for Sight PhD student. A.T.M. is funded by National Institute for Health Research UK (Moorfields Eye Hospital Biomedical Research Centre). Funding to pay the Open Access charge was provided by The Wellcome Trust.

REFERENCES

1. Nance, W.E., Warburg, M., Bixler, D. and Helveston, E.M. (1974) Congenital X-linked cataract, dental anomalies and brachymetacarpalia. *Birth Defects Orig. Artic. Ser.*, **10**, 285–291.
2. Horan, M.B. and Billson, F.A. (1974) X-linked cataract and Hutchinsonian teeth. *Aust. Paediatr.*, **10**, 98–102.
3. Walpole, I.R., Hockey, A. and Nicoll, A. (1990) The Nance-Horan syndrome. *J. Med. Genet.*, **27**, 632–634.
4. Lewis, R.A., Nussbaum, R.L. and Stambolian, D. (1990) Mapping X-linked ophthalmic diseases. IV. Provisional assignment of the locus for X-linked congenital cataracts and microcornea (the Nance-Horan syndrome) to Xp22.2–p22.3. *Ophthalmology*, **97**, 110–120.
5. Van Dorp, D.B. and Delleman, J.W. (1979) A family with X-chromosomal recessive congenital cataract, microphthalmia, a peculiar form of ear and dental anomalies. *J. Pediatr. Ophthalmol. Strabismus*, **16**, 166–171.
6. Seow, W.K., Brown, J.P. and Romaniuk, K. (1985) The Nance-Horan syndrome of dental anomalies, congenital cataracts, microphthalmia, and anteverted pinna—case report. *Pediatr. Dent.*, **7**, 307–311.
7. Toutain, A., Ayrault, A.D. and Moraine, C. (1997) Mental retardation in Nance-Horan syndrome: clinical and neuropsychological assessment in four families. *Am. J. Med. Genet.*, **71**, 305–314.
8. Bixler, D., Higgins, M. and Hartsfield, J. Jr. (1984) The Nance-Horan syndrome: a rare X-linked ocular–dental trait with expression in heterozygous females. *Clin. Genet.*, **26**, 30–35.
9. Stambolian, D., Lewis, R.A., Buetow, K., Bond, A. and Nussbaum, R. (1990) Nance-Horan syndrome: localization within the region Xp21.1–Xp22.3 by linkage analysis. *Am. J. Hum. Genet.*, **47**, 13–19.
10. Toutain, A., Dessay, B., Ronce, N., Ferrante, M.I., Tranchemontagne, J., Newbury-Ecob, R., Wallgren-Pettersson, C., Burn, J., Kaplan, J., Rossi, A. *et al.* (2002) Refinement of the NHS locus on chromosome Xp22.13 and analysis of five candidate genes. *Eur. J. Hum. Genet.*, **10**, 516–520.
11. Burdon, K.P., McKay, J.D., Sale, M.M., Russell-Eggitt, I.M., Mackey, D.A., Wirth, M.G., Elder, J.E., Nicoll, A., Clarke, M.P., FitzGerald, L.M. *et al.* (2003) Mutations in a novel gene, NHS, cause the pleiotropic effects of Nance-Horan syndrome, including severe congenital cataract, dental anomalies, and mental retardation. *Am. J. Hum. Genet.*, **73**, 1120–1130.
12. Brooks, S.P., Ebenezer, N.D., Poopalasundaram, S., Lehmann, O.J., Moore, A.T. and Hardcastle, A.J. (2004) Identification of the gene for Nance-Horan syndrome (NHS). *J. Med. Genet.*, **41**, 768–771.
13. Sharma, S., Ang, S.L., Shaw, M., Mackey, D.A., Gecz, J., McAvoy, J.W. and Craig, J.E. (2006) Nance-Horan syndrome protein, NHS, associates with epithelial cell junctions. *Hum. Mol. Genet.*, **15**, 1972–1983.
14. Ramprasad, V.L., Thool, A., Murugan, S., Nancarrow, D., Vyas, P., Rao, S.K., Vidhya, A., Ravishankar, K. and Kumaramanickavel, G. (2005) Truncating mutation in the NHS gene: phenotypic heterogeneity of Nance-Horan syndrome in an Asian Indian family. *Invest. Ophthalmol. Vis. Sci.*, **46**, 17–23.
15. Florijn, R.J., Loves, W., Maillette de Buy Wenniger-Prick, L.J., Mannens, M.M., Tijmes, N., Brooks, S.P., Hardcastle, A.J. and Bergen, A.A. (2006) New mutations in the NHS gene in Nance-Horan Syndrome families from the Netherlands. *Eur. J. Hum. Genet.*, **14**, 986–990.
16. Huang, K.M., Wu, J., Brooks, S.P., Hardcastle, A.J., Lewis, R.A. and Stambolian, D. (2007) Identification of three novel NHS mutations in families with Nance-Horan syndrome. *Mol. Vis.*, **13**, 470–474.
17. Reches, A., Yaron, Y., Burdon, K., Crystal-Shalit, O., Kidron, D., Malcov, M. and Tepper, R. (2007) Prenatal detection of congenital bilateral cataract leading to the diagnosis of Nance-Horan syndrome in the extended family. *Prenat. Diagn.*, **27**, 662–664.
18. Sharma, S., Burdon, K.P., Dave, A., Jamieson, R.V., Yaron, Y., Billson, F., Van Maldergem, L., Lorenz, B., Gecz, J. and Craig, J.E. (2008) Novel causative mutations in patients with Nance-Horan syndrome and altered localisation of the mutant NHS-A protein isoform. *Mol. Vis.*, **14**, 1856–1864.
19. Walsh, F.B. and Wegman, M.E. (1937) Pedigree of hereditary cataract, illustrating sex-limited type. *Bull. Johns Hopkins Hosp.*, **61**, 125–135.
20. Fraccaro, M., Morone, G., Manfredini, U. and Sanger, R. (1967) X-linked cataract. *Ann. Hum. Genet.*, **31**, 45–50.
21. Goldberg, M.F. and Hardy, J.M.B. (1971) X-linked cataract. In Bergsma, D. (ed.), *The Second Conference on the Clinical Delineation of Birth Defects. Part VIII. Eye*, Williams and Wilkins, Baltimore, **Vol. 3**, pp. 164–165.
22. Krill, A.E., Woodbury, G. and Bowman, J.E. (1969) X-chromosomal-linked sutural cataracts. *Am. J. Ophthal.*, **68**, 867–872.
23. Francis, P.J., Berry, V., Hardcastle, A.J., Maher, E.R., Moore, A.T. and Bhattacharya, S.S. (2002) A locus for isolated cataract on human Xp. *J. Med. Genet.*, **39**, 105–109.
24. Brooks, S., Ebenezer, N., Poopalasundaram, S., Maher, E., Francis, P., Moore, A. and Hardcastle, A. (2004) Refinement of the X-linked cataract locus (CXN) and gene analysis for CXN and Nance-Horan syndrome (NHS). *Ophthalmic Genet.*, **25**, 121–131.
25. Favor, J. and Pretsch, W. (1990) Genetic localisation and phenotypic expression of X-linked cataract (Xcat) in *Mus Musculus*. *Genet. Res.*, **56**, 157–162.
26. Stambolian, D., Favor, J., Silvers, W., Avner, P., Chapman, V. and Zhou, E. (1994) Mapping of the X-linked cataract (Xcat) mutation, the gene implicated in the Nance Horan syndrome, on the mouse X chromosome. *Genomics*, **22**, 377–380.
27. Huang, K.M., Wu, J., Duncan, M.K., Moy, C., Dutra, A., Favor, J., Da, T. and Stambolian, D. (2006) Xcat, a novel mouse model for Nance-Horan syndrome inhibits expression of the cytoplasmic-targeted Nhs1 isoform. *Hum. Mol. Genet.*, **15**, 319–327.

28. Bi, W., Sapir, T., Shchelochkov, O.A., Zhang, F., Withers, M.A., Hunter, J.V., Levy, T., Shinder, V., Peiffer, D.A., Gunderson, K.L. *et al.* (2009) Increased LIS1 expression affects human and mouse brain development. *Nat. Genet.*, **41**, 168–177.
29. Lee, J.A., Carvalho, C.M. and Lupski, J.R. (2007) A DNA replication mechanism for generating nonrecurrent rearrangements associated. *Cell*, **131**, 1235–1247.
30. Elgar, G., Sandford, R., Aparicio, S., Macrae, A., Venkatesh, B. and Brenner, S. (1996) Small is beautiful: comparative genomics with the pufferfish (*Fugu rubripes*). *Trends Genet.*, **12**, 145–150.
31. Niederreither, K., Vermot, J., Messaddeq, N., Schuhbaur, B., Chambon, P. and Dollé, P. (2001) Embryonic retinoic acid synthesis is essential for heart morphogenesis in the mouse. *Development*, **128**, 1019–1031.
32. Van Esch, H., Jansen, A., Bauters, M., Froyen, G. and Fryns, J.P. (2007) Encephalopathy and bilateral cataract in a boy with an interstitial deletion of Xp22 comprising the CDKL5 and NHS genes. *Am. J. Med. Genet. A.*, **143**, 364–369.
33. Silver, D.N., Lewis, R.A. and Nussbaum, R.L. (1987) Mapping the Lowe oculocerebrorenal syndrome to Xq24–q26 by use of restriction fragment length polymorphisms. *J. Clin. Invest.*, **79**, 282–285.
34. Craig, J.E., Friend, K.L., Gecz, J., Rattray, K.M., Troski, M., Mackey, D.A. and Burdon, K.P. (2008) A novel locus for X-linked congenital cataract on Xq24. *Mol. Vis.*, **14**, 721–266.
35. Peirson, S.N., Butler, J.N. and Foster, R.G. (2003) Experimental validation of novel and conventional approaches to quantitative real-time PCR data analysis. *Nucleic Acids Res.*, **31**, e73.